

Table II. The Effect of Various ^{11}B Decoupling Frequencies on the Proton Spectrum of $1,2\text{-(CH}_3)_2\text{B}_5\text{H}_7$

Decoupling radiofrequency	Boron atom irradiated	"Sharpening factor" ^a for methyl proton resonance		Other effects
		1 ^b	2 ^c	
Rf(X)	B(2)—CH ₃	1.4	2.1	Predominant effect on low-field bridge proton resonance. Little effect on terminal basal proton resonance
Rf(Y)	B(3,4,5)—H	1.4	1.8	Decouples base terminal protons and high-field bridge resonance. Little effect on low-field bridge resonance
Rf(Z)	B(1)—CH ₃	2.7	1.5	Little effect on terminal or bridge proton resonance
Rf(X) + rf(Y) + rf(Z)	B(1→5)	3.2	2.4	Spectrum totally decoupled

^a Sharpening factor = $(H_1/H_0) \times (W_0/W_1)$, where H_0 and W_0 = height, width at half-height of methyl resonance without applied ^{11}B decoupling; H_1 and W_1 = height, width at half-height of methyl resonance with applied ^{11}B decoupling. ^b 1 = high-field methyl resonance (shown to be apex). ^c 2 = low-field methyl resonance (shown to be basal).

tained by using three audiooscillators (X, Y, Z) which generated the corresponding decoupling radiofrequencies, rf(X, Y, Z). The effect of each individual frequency [rf(X → Z)] is also shown. Thus, for example, Figure 1d illustrates the effect of irradiating the basal borons B(3,4,5) which results in the collapse of the quartet (H— ^{11}B) and the concomitant appearance of a single peak. A simultaneous sharpening in the high-field bridge resonance is also noted.

The gross perturbations engendered in the thermal and bridge proton resonances are easily observed (Figure 1b–d), but the effect of ^{11}B irradiation upon the methyl resonances is a little less obvious. For purposes of comparing these effects we have defined a "sharpening factor" (Table II) which allows direct comparison between high- and low-field resonances. Careful examination of these data and the spectra allows the establishing of interdependence between the particular irradiating rf field and simultaneous effects on one or more regions of the spectrum. Thus it is seen that the low-field methyl and the low-field bridge resonances are decoupled by rf(X) (Figure 1c); similarly interrelated are the terminal proton and the high-field bridge resonances (Figure 1d), whereas the high-field methyl peak appears to be predominantly independent, Figure 1e. These effects undoubtedly result from the proximity of these proton environments to the irradiated boron atoms. These results provide confirmation of the boron assignments and enable the proton resonances to be assigned. Details are presented in Table III.

Table III. ^1H Nmr Chemical Shift Values and Coupling Constants for $1,2\text{-(CH}_3)_2\text{B}_5\text{H}_7$

Proton environment ^a	τ , ppm ^b	J , Hz ^c
H···B(3,5) ^d	7.66	156
H···B(4)		
H μ (2,5)	11.45	~30 ^e
H μ (3,4)	12.05	~30 ^e
H···C(1)	9.95	
H···C(2)	9.60	

^a B(3,4,5) are basal borons; H μ = bridge hydrogen, H μ (2) designates bridge proton between boron atoms 2 and 3, etc. ^b To avoid negative values, τ (TMS = 10.00) is used rather than δ . ^c H— ^{11}B coupling only. ^d No chemical shift difference discernible. ^e Cannot be accurately determined due to lack of fine structure.

It is apparent from the data in Table II and by observation of the spectra that there is some overlap of effect.

For example, although the primary effect of rf(X) is to decouple boron atom B(2), thus sharpening the base methyl resonance and the low-field bridge resonance, it also has some effect upon the rest of the spectrum causing a slight sharpening in the apex methyl resonances and altering the coupling constants of the basal B–H resonances. This is almost certainly due to the band width of the irradiating field (*vide supra*) but may be also due, in part, to small long-range coupling effects.

Despite this slight element of uncertainty, it is encouraging to note the success of this method in that it has enabled the broad bridge proton resonance to be decoupled and assigned. The definitive assignment of the methyl proton resonances has also been possible; and further, from these and other experiments on various pentaborane derivatives,³ conclusions have been made regarding the effect of substituents upon the chemical shift of the bridge resonances. Thus taking the values in pentaborane as a standard for reference, a basal methyl or ethyl group shifts the resonance due to the adjacent equivalent protons, H μ (2,5), downfield by *ca.* 0.7 ppm, without substantially affecting the far bridge resonance, H μ (3,4). A base chlorine atom caused a similar downfield shift of *ca.* 1.5 ppm, again without great effect upon the far resonance. In poly-substituted derivatives these affects appear to be additive.

Philip M. Tucker, Thomas Onak

Department of Chemistry
California State College at Los Angeles
Los Angeles, California 90032

Received July 14, 1969

Organometallic Conformational Equilibria. VIII. Spin Saturation Labeling Studies of the Epimerization and Isomerization Mechanism of 1,2,3-Trihapto-(3-acetyl-2-methylallyl)[(S)- α -phenethylamine]-chloropalladium(II)¹

Sir:

Crystallization of 1,2,3-trihapto(3-acetyl-2-methylallyl)[(S)- α -phenethylamine]chloropalladium(II)² from carbon tetrachloride results in the isolation of only one

(1) Part VII: J. W. Faller and M. J. Incurvia, *J. Organometal. Chem.*, in press.

(2) This nomenclature has been suggested by Cotton.³ The Greek prefix *hapto* indicates the number and location of carbon atoms connected to the metal atom.

(3) F. A. Cotton, *J. Am. Chem. Soc.*, **90**, 6230 (1968).

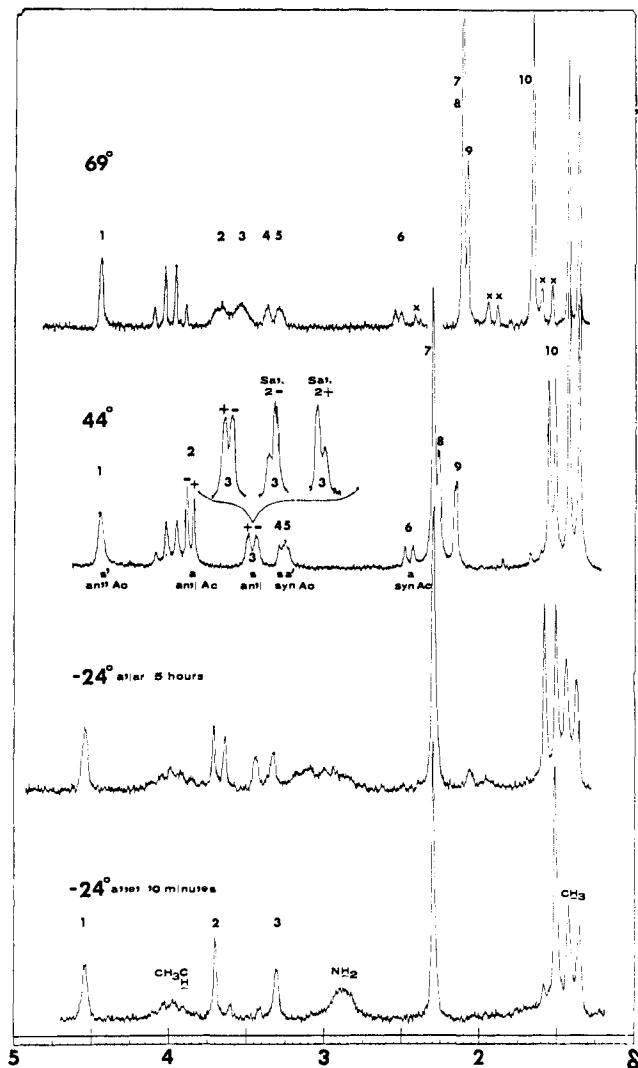


Figure 1. Pmr spectra (100 MHz) of 1,2,3-*trihapto*(3-acetyl-2-methyl)l[(*S*)- α -phenethylamine]chloropalladium(II) in deuteriochloroform-benzene solution. The lower -24° spectrum was taken 10 min after the solid was added to a deuteriochloroform-benzene (5:1) solution at -50° . The 3:1 deuteriochloroform-benzene solution (44°) and the 5:1 solution (69°) were treated with D_2O to reduce the intensity of the amine proton resonances. The resonances marked with an "x" in the 69° spectrum are decomposition products. The insert in the 44° spectrum shows the effects on the components of resonance 3 upon saturation of the component resonances of 2. The resonance at δ 1.4 ($J \cong 7$ Hz) arises from the methyl group in the amine.

of the possible diastereoisomers.⁴ When these crystals are dissolved, epimerization to a 1:1 mixture of diastereoisomers appears to occur. Polarimetric rate studies have indicated an activation energy of 20.4 kcal/mole for the process.⁵ Several mechanisms have been proposed to explain these observations, as well as other effects arising from isomerization reactions of π -allyl complexes, but no clear-cut conclusions have been reached. We present here pmr studies which allow us to determine the predominant mechanism for epimerization and isomerization.

(4) P. Corradini, G. Maglio, A. Musco, and G. Paiaro, *Chem. Commun.*, 618 (1966).

(5) F. DeCandia, G. Maglio, A. Musco, and G. Paiaro, *Inorg. Chim. Acta*, 2, 333 (1968).

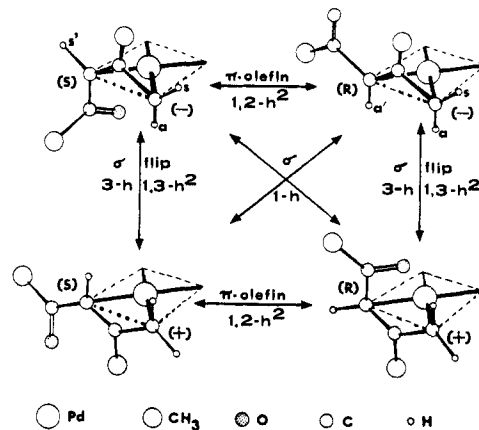


Figure 2. Modes of interconversion of the various diastereoisomers.

The pmr spectrum of a 5:1 deuteriochloroform-benzene solution of the complex prepared at -50° shows the five resonances expected for the allylic moiety in addition to the signals arising from the amine (Figure 1). When the temperature was raised to -20° , five new resonances gradually appeared in the spectrum. At still higher temperatures, ten more resonances grew in, until the pmr spectrum generally observed at room temperature was obtained (Figure 1). Determination of the rate of appearance of the first set of five resonances at several temperatures yielded rate constants within experimental error of those measured polarimetrically for the epimerization.⁶ Clearly the first set of resonances to grow in should be assigned to the epimer of the complex in the crystalline material, whereas the second set of resonances to appear are presumably a pair of epimers of a different geometrical isomer.⁶

Confining attention to the π -allylic moiety,⁷ one notes that two geometrical isomers are possible, both of which are chiral (Figure 2). Assignment of the *anti*-acetyl configuration to the diastereoisomer present in the solid and hence the major isomer in solution was made on the basis of coupling between resonances 1 and 3 indicative of the presence of two *syn* protons, comparison of chemical shifts with model compounds, and nuclear Overhauser effects.⁸

(6) The rates of epimerization obtained by pmr were ($^\circ C, \times 10^{-3}/sec$): $-15.9, 0.92$; $-13.4, 1.55$; and $-11.8, 1.81$, giving $\Delta F_1^* \sim 18.5$ kcal/mole. From the rates of isomerization one obtains $\Delta F_2^* \sim 21.2$ kcal/mole. From line broadening we estimate $\Delta F_3^* \sim 18.8$ kcal/mole for epimerization of the second isomer.

(7) While *cis-trans* isomerism of the amine with respect to the acetyl group is possible and indeed has been observed for various pyridine derivatives of π -crotylpalladium complexes,¹ we do not observe this phenomenon here. It appears that at least 90% of the complex is present in solution in the *trans* (or possibly the *cis*) form. Some broadening of the peaks at low temperature is observed especially in the minor isomer, but no resonances attributable to the other isomer have been discerned. This isomerism does not influence our results because at no time would interconversion of the *cis-trans* isomers lead to inversion of the chirality in the π -allylpalladium moiety.

(8) *syn-syn* coupling is much greater than *syn-anti* or *anti-anti* coupling and is present in most π -allyl(amine)palladium complexes.⁹ The (*R*)(*S*)- α -phenethylamine-1,2,3-*trihapto*(3-acetylallyl) complex exists almost entirely as the *syn*-acetyl isomer as indicated by the pmr: δ 5.81, multiplet, central proton; δ 3.79, doublet (7.5 Hz), *syn* proton; δ 3.57, doublet (11.0 Hz), *anti*-proton; δ 2.82, doublet (12.8 Hz), *anti* proton; δ 2.29, singlet, acetyl methyl. The lower field *anti*-proton resonance is assigned to the *anti* proton adjacent to the acetyl group on the basis of the shielding expected from the carbonyl group. Since the resonances of this complex are in the same region as those of the minor isomer of the 3-acetyl-2-methyl complex, and since the temperature dependence of the pmr spectra closely parallels that of the minor isomer, the assignment of the minor isomer of the 3-acetyl-2-methyl complex as the *syn*-Ac isomer tends to be confirmed. Similar *syn-anti* geometrical

Thus the assignments (see Figures 1 and 2) for the *anti*-acetyl isomer are as follows: (1) to the *syn* proton adjacent to the acetyl group, H_{s'}; (2) to the *anti* proton, H_a; (3) to the *syn* proton, H_s; and the methyl resonances at δ 2.3 and 1.5 to the acetyl and to the allyl methyl group, respectively. The resonances of the *syn*-acetyl isomer were assigned similarly, as indicated in Figure 1.

In the absence of a chiral amine, one would expect only ten resonances to be associated with the acetyl-methylallyl moieties, five for each geometrical isomer. But a chiral amine, *i.e.*, (*S*)- α -phenethylamine, produces epimers which show only slight differences in chemical shifts; hence, in Figure 1 regions of the spectrum are labeled 1 to 10, but each labeled region contains two component resonances, one for each epimer.¹¹

When the temperature was raised above 50°, resonances 1, 2, 3, 7, and 10 began to broaden. At 73°, resonances 2 and 3 appeared to coalesce to a broad single peak, whereas the pairs of components of 1, 7, and 10 had coalesced to single resonances. Above 55°, resonances 4 and 6 began to broaden and the components of the remaining resonances coalesced. Severe decomposition of the complex occurred above these temperatures; hence, reliable data on further broadening and coalescence could not be obtained. Nevertheless, indirect spin saturation experiments,¹² which effectively allow labeling of given proton positions and will be discussed for one example below, indicated that resonances 1 and 5, and 9 and 10 were exchanging, but at a somewhat slower rate than were 4 and 6.

On the basis of the assignments discussed earlier, the first phase of temperature dependence corresponds to epimerization of the major isomer, *anti*-Ac, as indicated by the disappearance of the pair of components in resonance 10 and averaging of the *syn* and *anti* protons. The second phase corresponds to epimerization of the minor isomer, as indicated by the averaging of the *syn* and *anti* protons and the coalescence of components. Finally, the third phase is due to isomerization, since the resonances of both isomers are interchanging.

The averaging which is observed will allow a distinction to be made among all of the mechanisms which have been previously proposed for averaging of *syn* and *anti* protons in π -allyl complexes. For simplicity we will assume that the isomer in the solid is the (*S*)-*anti*-Ac complex.¹³ Hence, in this instance, H_a and H_s would be in a (−) absolute configuration (as defined previously¹⁴). Therefore, the adjacent resonances which appeared at the same rate as epimerization must be assigned to H_a and H_s in the (+) absolute configuration.

Generally three types of mechanisms have been sug-

isomerism is exhibited by the π -allylic palladium chloride complexes formed through the decarboxylation of malonic acid derivatives.¹⁰ These assignments are further substantiated by Overhauser effect studies, which will be discussed in detail in a future publication.

(9) J. W. Faller and M. J. Incurvia, unpublished results.

(10) R. Hüttel and H. Schmid, *Chem. Ber.*, **101**, 252 (1968).

(11) The components of each resonance are not clearly visible in this solvent; however, by appropriate changes of solvent, the components of each resonance become clearly visible.

(12) B. M. Fung, *J. Chem. Phys.*, **47**, 1409 (1967), and references therein.

(13) The absolute configuration is irrelevant in this discussion of the pmr spectrum. If the opposite configuration were found in the solid, one could readily adapt the same discussion by considering the (*R*)- α -phenethylamine derivative rather than the (*S*).

(14) J. W. Faller, M. J. Incurvia, and M. E. Thomsen, *J. Am. Chem. Soc.*, **91**, 518 (1969), and references therein.

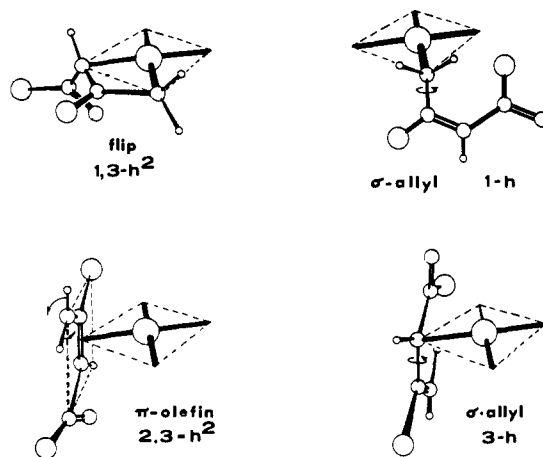


Figure 3. Possible intermediates for some of the proposed mechanisms.

gested: a 1,3-*h*² flip, wherein the allyl moiety becomes coplanar with the palladium atom;¹⁵ a *h*²-olefin intermediate, which allows free rotation of the uncoordinated end;¹⁴ and a σ -bonded intermediate.^{4,5,14} Some of these intermediates are shown in Figure 3, and the interconversions which occur are depicted in Figure 2. Each of these mechanisms involves exchange of different proton sites, and they are summarized in Table I.

Table I. Site Interchanges Required by Different Mechanisms

	$(S)\text{-anti-Ac} \xrightleftharpoons{k_1} (R)\text{-anti-Ac}$					
	$(S)\text{-syn-Ac} \xrightleftharpoons{k_2} (R)\text{-syn-Ac}$					
	$(S)\text{-anti-Ac} \xrightleftharpoons{k_3} (S)\text{-syn-Ac}$					
	$(R)\text{-anti-Ac} \xrightleftharpoons{k_3} (R)\text{-syn-Ac}$					
	$k_1 \gtrsim k_2 \gg k_3$					
		1,3- <i>h</i> ² flip	1- <i>h</i> σ -allyl	3- <i>h</i> σ -allyl	2,3- <i>h</i> ² π -olefin	1,2- <i>h</i> ² π -olefin
(<i>S</i>)- <i>anti</i> -Ac						
H ₁	s(−)	a(+)	a(+)	s(+)	a(−)	s(−)
H ₂	a(−)	s(+)	s(+)	a(+)	s(−)	a(−)
H ₃	s'(S)	a'(R)	s'(R)	a'(S)	s'(S)	a'(S)
Me	<i>anti</i> (S)	<i>syn</i> (S)	<i>anti</i> (R)	<i>syn</i> (S)	<i>anti</i> (S)	<i>syn</i> (R)
Ac	<i>anti</i> (S)	<i>syn</i> (S)	<i>anti</i> (R)	<i>syn</i> (S)	<i>anti</i> (S)	<i>anti</i> (R)

The 1,3-*h*² flip mechanism is inconsistent with the data because we do not observe broadening of the *syn* (s) and *anti* (a) proton resonances along with simultaneous broadening of the *syn* (s') and *anti* (s') resonances of the proton adjacent to the acetyl group. In particular, the distinguishing feature of an end rotation (2,3-*h*² intermediate) mechanism in comparison to a σ -bonded intermediate mechanism is the retention of configuration in the former and the inversion of configuration in the latter. Hence, for the first process one may distinguish the mechanisms by observing the mode of exchange of the component resonances 2 and 3. At 44°, a temperature at which $k_1 > 1/T_1(H_a)$, saturation of the lower component of resonance 2, *i.e.*, the *anti* proton in the (−) configuration, caused a decrease in the intensity

(15) The planar flip mechanism could occur either with or without^{5,14} interchange of *syn* and *anti* sites.

of the lower component of resonance 3, *i.e.*, the *syn* proton in the (+) configuration. Therefore, inversion of configuration occurs with *syn-anti* interchange, and a σ -bonded intermediate (1-*h*) is implied for the first epimerization process of the *anti*-Ac complex. Similarly, spin saturation labeling experiments and observation of coalescences allow us to conclude that a 1-*h* σ -bonded intermediate is primarily responsible for epimerization of the *syn*-Ac complex. Furthermore, isomerization appears to occur predominantly *via* a 3-*h* σ -bonded intermediate.

Acknowledgment. We wish to acknowledge the financial support of the Connecticut Research Commission and the Petroleum Research Fund administered by the American Chemical Society. We wish to thank the National Science Foundation for Grant GP-6938 which allowed the purchase of the Varian HA-100 spectrometer.

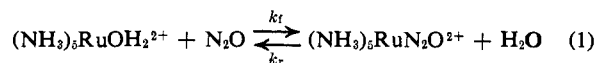
J. W. Faller, M. E. Thomsen
Department of Chemistry, Yale University
New Haven, Connecticut 06520
Received June 23, 1969

Formation and Reactions of $[(\text{NH}_3)_5\text{RuN}_2\text{O}^{2+}]$

Sir:

When N_2O is added to an aqueous solution of $(\text{NH}_3)_5\text{-RuOH}_2^{2+}$, produced by reduction of $(\text{NH}_3)_5\text{RuCl}^{2+}$ by Cr^{2+} , Pt-H_2 , or Zn(Hg) , a new absorption band develops having a maximum at 238 nm (see Figure 1). It increases in intensity when the concentration of N_2O increases, disappears when N_2O is removed by passing argon through the solution, and is restored when N_2O is again added. The rate at which the absorption grows can conveniently be measured spectrophotometrically. Plots of $\ln(A_\infty - A_t)$ vs. t are found to be strictly linear up to at least 95% completion of reaction. In Figure 2 the values of k_{obsd} as they are obtained from the plots are shown as a function of N_2O concentration.

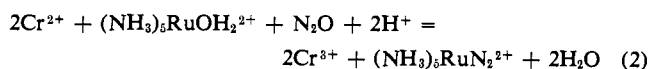
The data of Figure 2 show that k_{obsd} is given by the relation $k_1 + k_2[\text{N}_2\text{O}]$. The general observations described above and the kinetic data can be interpreted on the basis that N_2O associates reversibly with $(\text{NH}_3)_5\text{-RuOH}_2^{2+}$.



On the basis of this interpretation, the rate of approach to equilibrium at constant concentration of N_2O should follow pseudo-first-order behavior, and, moreover, the first-order specific rate k_{obsd} should be given by $k_r + k_f[\text{N}_2\text{O}]$ (assuming, that is, that the rate laws of the forward and reverse reactions are as indicated in eq 1). Identifying $k_1 (= 1.35 \times 10^{-3} \text{ sec}^{-1})$ with k_r and $k_2 (= 9.5 \times 10^{-3} \text{ M}^{-1} \text{ sec}^{-1})$ with k_f , K_1 for reaction 1 at 6.8° and $\mu = 0.023$ (Cl^- as anion) is calculated as 7.0 (using $\text{N}_2\text{O(aq)}$ rather than $\text{N}_2\text{O(g)}$ as the standard state for this reactant). It should be noted that the k_r term makes by far the greater contribution to k_{obsd} , and thus the value of k_r is rather well defined by the data. The coefficient k_f is obtained from the slope of the line in Figure 2 and is, therefore, less well defined. The value of k_f suggested by the above data is, however, confirmed

by an independent measurement which will now be described.

When Cr^{2+} is present in a solution containing both $(\text{NH}_3)_5\text{RuOH}_2^{2+}$ and N_2O , the reaction



takes place quantitatively. The kinetics of reaction 2 are of particular interest. Though Cr^{2+} is consumed, the reaction rate does not depend on $[\text{Cr}^{2+}]$, and the rate law for the reaction is given by

$$\frac{d[(\text{NH}_3)_5\text{RuN}_2^{2+}]}{dt} = k[(\text{NH}_3)_5\text{RuOH}_2^{2+}][\text{N}_2\text{O}] \quad (3)$$

Good kinetic data were obtained following the growth of the nitrogen complex spectrophotometrically at 221 nm. In determining the rate law, N_2O was in excess, but the initial concentration covered the range 8.38×10^{-3} – $4.52 \times 10^{-2} \text{ M}$ for the series.¹ Chromous ion covered the range 1.2×10^{-4} to $1.2 \times 10^{-3} \text{ M}$; the initial concentration of Ru(II) was fixed at $6 \times 10^{-5} \text{ M}$. The coefficient k at 6.8° is found to be $10.1 \times 10^{-3} \text{ M}^{-1} \text{ sec}^{-1}$. The form of rate law 3 and the excellent agreement of k with k_f shows that the rate of formation of the N_2O complex is rate determining for reaction 2 and this, in turn, suggests that the N_2O complex is reduced virtually as rapidly as it is formed.

The stoichiometry for reaction 2 was checked covering the range $[\text{Cr}^{2+}]/[\text{Ru(II)}]$ from 1.2 to 10.0 by using Fe^{3+} to quench the reaction, and then developing the color of Fe^{2+} with *o*-phen.² Under our conditions, the oxidation by Fe^{3+} of the nitrogen complex was slow compared to that of Cr^{2+} or $(\text{NH}_3)_5\text{RuOH}_2^{2+}$. By waiting 1 hr after the Fe^{3+} was added, the nitrogen complex was destroyed quantitatively, and the amount of nitrogen liberated was determined by gas chromatography using this reaction. Within the limits of accuracy of the methods, $\pm 5\%$, the agreement with requirements of eq 2 was exact. The first method was also used to follow the rate of reaction, again in satisfactory agreement with the rates determined spectrophotometrically.

The kinetic measurements were repeated at 20.1° . At the higher temperature, k_r contributes proportionately even more to k_{obsd} than at the lower, and, as before, rather accurate value of this parameter can be obtained. The value of k_f was determined by measuring the rate of reaction 2 at the higher temperature. The values of k_r and k_f obtained, $9.1 \pm .5 \times 10^{-3} \text{ sec}^{-1}$ and $4.51 \times 10^{-2} \text{ M}^{-1} \text{ sec}^{-1}$, respectively ($\mu = 0.02$ with Cl^-), combine to yield K_1 at 20.1° as 5.0.

The affinity of $(\text{NH}_3)_5\text{RuOH}_2^{2+}$ for N_2O was also determined by a vacuum-line method,³ comparing the partial pressure of N_2O over a solution containing $(\text{NH}_3)_5\text{RuOH}_2^{2+}$ with that registered in a blank experiment identical in every respect, but with sodium chloride replacing the ruthenium complex. K_1 was measured as 8.3 at 24° and 8.6 at 22° . Because the pressure changes recorded are very small, and because

(1) The concentration of N_2O in solution was determined using the value of Henry's law constant as obtained from "International Critical Tables," Vol. III, McGraw-Hill Book Co., Inc., New York, N. Y., 1928, p 259.

(2) T. J. Meyer and H. Taube, *Inorg. Chem.*, 7, 2369 (1968); G. Charlot, "Colorimetric Determination of Elements," Elsevier Publishing Co., New York, N. Y., 1964, p 274.

(3) The authors wish to express their appreciation to Mr. P. R. Jones for his assistance with the vacuum-line work.